

# Correlation-based color mosaic interpolation using a connectionist approach

Gary L. Embler\*

Agilent Technologies, Inc.  
3175 Bowers Avenue, MS 87H  
Santa Clara, California 95054  
USA

## ABSTRACT

This paper presents a specialized extension of a general correlation-based interpolation paradigm, for interpolating image sample color values obtained through a color filter mosaic. This extension features a kernel determined from a priori assumed image characteristics in the form of pre-defined (as opposed to learned) local sample neighborhood patterns. The interpolation procedure locally convolves the color-filtered image samples with the kernel to obtain the interpolated color values. The kernel establishes a mapping from the color-filtered input values to the recovered color output values using weighted, ordered, and thresholded sums of sample values from the local sample neighborhood. This mapping attempts to exploit local image sample interdependencies in order to preserve detail, while minimizing artifacts. The procedure is simulated for the Bayer RGB color filter mosaic using a quasi-linear connectionist architecture that is real-time-hardware-implementable. A perceptual comparison of images obtained from this interpolation with images obtained from bilinear interpolation shows a visible reduction in interpolation artifacts.

Keywords: Demosaicing, color interpolation, image interpolation, image reconstruction, superresolution, Bayer color filter array, connectionist architecture, neural network.

## 1. INTRODUCTION

Image sample interpolation is well established as an ill-posed or under-constrained problem with no unique solution.<sup>1</sup> However, images of natural scenes typically have common characteristics that aid in obtaining a desirable interpolation solution.

Color mosaic interpolation is a special case of image sample interpolation, where the interpolation nominally applies to the same-color samples in the mosaic. Existing color mosaic interpolation approaches use static reconstruction theory-based methods (*e.g.*, bilinear interpolation), or dynamic adaptive methods (*e.g.*, direction-adaptive bilinear interpolation).<sup>2, 3, 4, 5, 6, 7, 8</sup> These methods make various assumptions about image characteristics, such as the assumption that neighboring image samples will show some degree of smoothness.

---

\* [gembler@inspirics.com](mailto:gembler@inspirics.com); phone 1 408 970-2537; fax 1 408 970-2416; this paper and supplemental materials (image files and MATLAB® code) are at <http://www.inspirics.com/publications/>.

Copyright 2002 Society of Photo-Optical Instrumentation Engineers.  
This paper will be published in Proceedings of SPIE Vol. 4669 and is made available as an electronic preprint with permission of SPIE. One print or electronic copy may be made for personal use only. Systematic or multiple reproduction, distribution to multiple locations via electronic or other means, duplication of any material in this paper for a fee or for commercial purposes, or modification of the content of the paper are prohibited.

Images of natural scenes are known to have local luminance interdependencies. This trait may be exploited for interpolating image samples to obtain higher image resolutions.<sup>9, 10, 11</sup> Go *et al.* present an extension to this paradigm for interpolating image color sample values obtained from a color filter mosaic.<sup>12</sup> This paper proposes another approach to this color mosaic interpolation method, derived from assumptions about expected image characteristics. These assumptions serve to facilitate real-time hardware implementation of the interpolation procedure, while still offering better image quality than image quality obtainable from bilinear interpolation.

## 2. METHODOLOGY FOR COLOR MOSAIC INTERPOLATION

The proposed methodology makes the following assumptions regarding image characteristics:

- Different local sample neighborhoods within images can share similar patterns.
- For the similar local patterns mentioned above, the patterns are similar across different scales.

These assumptions allow a priori information from local sample patterns to be used in obtaining interpolated color values. According to these assumptions, patterns of high-resolution neighborhoods (sample neighborhoods with all color values present) are similar to patterns of the corresponding low-resolution neighborhoods (color mosaic sample neighborhoods; *i.e.*, the inputs to the interpolation).

In order to use this methodology, the local sample patterns and their mapping to the corresponding interpolated color values must be defined. This information could either be learned from available data (*e.g.*, sampled images) as in Ref. 10, or derived from assumptions about expected image characteristics. This paper is concerned with the later approach. The following assumptions are made:

- A small, odd-number dimensioned, square spatial sample neighborhood (*e.g.*, 3 x 3 samples) centered on the color output value location, is sufficient for the local sample neighborhood size and configuration.
- The set of local neighborhood sample patterns may be derived from combinations of minimum and maximum sample values in the local neighborhood. These patterns represent various luminance gradient configurations in the local neighborhood.
- The local neighborhood bilinear-interpolated color value may be used as a starting color output value.
- The starting color output value (*i.e.*, the bilinear-interpolated value) may be adjusted based on the similarity of its local neighborhood sample values to the set of sample pattern values. The adjustment amount is proportional to the luminance gradient (as represented by the patterns), and the adjustment direction (increase or decrease) is made in the direction towards the center sample value. At the maximum adjustment amount (corresponding to the maximum luminance gradient), the color output value is made equal to the center sample value.

This procedure attempts to take into account an assumed correlation between the local neighborhood sample values and the expected center color values. This procedure also attempts to improve perceptual quality by driving the overall center color towards a more neutral tone, thus minimizing the perception of chromatic aliasing artifacts (“color fringes”) near large luminance gradients.

The local sample patterns are determined from combinations of minimum and maximum local sample values. For each different pattern of minimum and maximum local sample values, a desired color output value (minimum or maximum) is assigned. This assignment is made based on the rules above; *i.e.*, equal to the center sample value for patterns with large luminance gradients. For the Bayer RGB color mosaic<sup>13</sup>, patterns arising from the following two sources are used to determine approximately the luminance gradients’ configuration and amount:

- Different combinations of the green samples’ minimum and maximum values.
- Different combinations of the minimum and maximum values of samples the same color as the center color being interpolated.

For interpolating green, only patterns arising from the green samples' minimum and maximum values are used, due to the high perceptual correlation of green with image luminance.<sup>14</sup>

To determine approximately each pattern's degree and direction of adjustment to the bilinear-interpolated color values, the pre-assigned output value for each pattern is compared with the bilinear-interpolated value for the same pattern. The approximate degree and direction of adjustment is the difference between the pre-assigned value and the bilinear-interpolated value. This difference determines the approximate weighting factors for the mapping of the patterns' sample values to the color output values, through the adjustment of the bilinear-interpolated starting values.

For an  $N \times N$ -element mosaic, where  $N$  is an odd integer, the procedures of this methodology are of the general form

$$\hat{x} = f(x[n_1, n_2]) = \begin{cases} \bar{x} - \tilde{x}_{neg} & \text{if } \bar{x} > x_{cent} \text{ and } \bar{x} - \tilde{x}_{neg} > x_{cent}, \\ \bar{x} + \tilde{x}_{pos} & \text{if } \bar{x} < x_{cent} \text{ and } \bar{x} + \tilde{x}_{pos} < x_{cent}, \text{ or} \\ x_{cent} & \text{otherwise} \end{cases}, \quad (1)$$

where  $\hat{x}$  is the interpolated color value for the local neighborhood center,  $x[n_1, n_2]$ , where  $n_1, n_2 = 0, 1, \dots, N-1$ , is the local neighborhood sample value 2D array,  $\bar{x}$  is the local neighborhood bilinear-interpolated center value,  $\tilde{x}_{neg}$  and  $\tilde{x}_{pos}$  are, respectively, the local-neighborhood-based negative and positive adjustments to the bilinear-interpolated center value, and  $x_{cent} = x\left[\frac{N-1}{2}, \frac{N-1}{2}\right]$  is the local neighborhood center sample value.

Forms for individual red, green, and blue interpolated color values of a Bayer color filter mosaic are

$$\hat{x}_{red} = \begin{cases} \bar{x}_{red} - \tilde{x}_{negred} & \text{if } \bar{x}_{red} > x_{cent} \text{ and } \bar{x}_{red} - \tilde{x}_{negred} > x_{cent}, \\ \bar{x}_{red} + \tilde{x}_{posred} & \text{if } \bar{x}_{red} < x_{cent} \text{ and } \bar{x}_{red} + \tilde{x}_{posred} < x_{cent}, \text{ or} \\ x_{cent} & \text{otherwise} \end{cases}, \quad (2)$$

$$\hat{x}_{gm} = \begin{cases} \bar{x}_{gm} - \tilde{x}_{neggm} & \text{if } \bar{x}_{gm} > x_{cent} \text{ and } \bar{x}_{gm} - \tilde{x}_{neggm} > x_{cent}, \\ \bar{x}_{gm} + \tilde{x}_{posgm} & \text{if } \bar{x}_{gm} < x_{cent} \text{ and } \bar{x}_{gm} + \tilde{x}_{posgm} < x_{cent}, \text{ or} \\ x_{cent} & \text{otherwise} \end{cases}, \quad (3)$$

$$\hat{x}_{blu} = \begin{cases} \bar{x}_{blu} - \tilde{x}_{negblu} & \text{if } \bar{x}_{blu} > x_{cent} \text{ and } \bar{x}_{blu} - \tilde{x}_{negblu} > x_{cent}, \\ \bar{x}_{blu} + \tilde{x}_{posblu} & \text{if } \bar{x}_{blu} < x_{cent} \text{ and } \bar{x}_{blu} + \tilde{x}_{posblu} < x_{cent}, \text{ or} \\ x_{cent} & \text{otherwise} \end{cases}, \quad (4)$$

where  $\hat{x}_{red}$ ,  $\hat{x}_{gm}$ ,  $\hat{x}_{blu}$  are the final interpolated red, green, and blue values,  $\bar{x}_{red}$ ,  $\bar{x}_{gm}$ ,  $\bar{x}_{blu}$  are bilinear-interpolated red, green, and blue values, and  $\tilde{x}_{negred}$ ,  $\tilde{x}_{posred}$ ,  $\tilde{x}_{neggm}$ ,  $\tilde{x}_{posgm}$ ,  $\tilde{x}_{negblu}$ ,  $\tilde{x}_{posblu}$  are red, green, and blue negative and positive adjustments to the bilinear-interpolated values.

The negative and positive adjustment values  $\tilde{x}_{neg}$  and  $\tilde{x}_{pos}$  are

$$\tilde{x}_{neg} = \max_d [w_{negpat_d} f_{negpat_d}(x)] \quad , \quad (5)$$

$$\tilde{x}_{pos} = \max_d [w_{pospat_d} f_{pospat_d}(x)] \quad , \quad (6)$$

where  $d = 0, 1, \dots, D - 1$  is the pattern dimension index,  $w_{negpat_d}$  and  $w_{pospat_d}$  are adjustment weights for negative and positive adjustments, and  $f_{negpat_d}(x)$  and  $f_{pospat_d}(x)$  are negative and positive adjustment functions of local neighborhood sample patterns.

Forms for individual red, green, and blue negative and positive adjustment values of a Bayer color filter mosaic are

$$\tilde{x}_{negred} = \max_d [w_{negredpat_d} f_{negredpat_d}(x)] \quad , \quad (7)$$

$$\tilde{x}_{posred} = \max_d [w_{posredpat_d} f_{posredpat_d}(x)] \quad , \quad (8)$$

$$\tilde{x}_{neggrn} = \max_d [w_{neggrmpat_d} f_{neggrmpat_d}(x)] \quad , \quad (9)$$

$$\tilde{x}_{posgrn} = \max_d [w_{posgrmpat_d} f_{posgrmpat_d}(x)] \quad , \quad (10)$$

$$\tilde{x}_{negblu} = \max_d [w_{negblupat_d} f_{negblupat_d}(x)] \quad , \quad (11)$$

$$\tilde{x}_{posblu} = \max_d [w_{posblupat_d} f_{posblupat_d}(x)] \quad , \quad (12)$$

where  $w_{negredpat_d}$ ,  $w_{posredpat_d}$ ,  $w_{neggrmpat_d}$ ,  $w_{posgrmpat_d}$ ,  $w_{negblupat_d}$ ,  $w_{posblupat_d}$ ,  $f_{negredpat_d}(x)$ ,  $f_{posredpat_d}(x)$ ,  $f_{neggrmpat_d}(x)$ ,  $f_{posgrmpat_d}(x)$ ,  $f_{negblupat_d}(x)$ ,  $f_{posblupat_d}(x)$  are adjustment weights and functions of local neighborhood sample patterns for red, green, and blue interpolation.

The local neighborhood sample pattern functions are

$$f_{negpat_d}(x) = \begin{cases} \max[f_{neg_d}(x) + f_{neg_d}(x_{grn}) + f_{neg_d}(x_{cent})] - b_d & \text{if } \max[\cdot] > b_d, \text{ or} \\ 0 & \text{otherwise} \end{cases} \quad , (13)$$

$$f_{pospat_d}(x) = \begin{cases} \max[f_{pos_d}(x) + f_{pos_d}(x_{grn}) + f_{pos_d}(x_{cent})] - b_d & \text{if } \max[\cdot] > b_d, \text{ or} \\ 0 & \text{otherwise} \end{cases} \quad , (14)$$

where  $b_d$  is an activation threshold bias term,  $f_{neg_d}(x)$  and  $f_{pos_d}(x)$  are functions of the local neighborhood samples the same color as the color being interpolated (except green samples),  $f_{neg_d}(x_{grn})$  and  $f_{pos_d}(x_{grn})$  are functions of the local neighborhood green samples (except a center sample), and  $f_{neg_d}(x_{cent})$  and  $f_{pos_d}(x_{cent})$  are functions of the center sample (red, green, or blue). Note that the bias term  $b_d$  performs a variable activation thresholding function, with  $f_{negpat_d}(x)$ ,  $f_{pospat_d}(x) > 0$  only if  $\max[\cdot] > b_d$ .

The local neighborhood sample pattern functions for red, green, and blue interpolation are

$$f_{negredpat_d}(x) = \begin{cases} \max[f_{neg_d}(x_{red}) + f_{neg_d}(x_{grn}) + f_{neg_d}(x_{cent})] - b_d & \text{if } \max[\cdot] > b_d, \text{ or} \\ 0 & \text{otherwise} \end{cases}, (15)$$

$$f_{posredpat_d}(x) = \begin{cases} \max[f_{pos_d}(x_{red}) + f_{pos_d}(x_{grn}) + f_{pos_d}(x_{cent})] - b_d & \text{if } \max[\cdot] > b_d, \text{ or} \\ 0 & \text{otherwise} \end{cases}, (16)$$

$$f_{neggrmpat_d}(x) = \begin{cases} \max[f_{neg_d}(x_{grn}) + f_{neg_d}(x_{cent})] - b_d & \text{if } \max[\cdot] > b_d, \text{ or} \\ 0 & \text{otherwise} \end{cases}, (17)$$

$$f_{posgrmpat_d}(x) = \begin{cases} \max[f_{pos_d}(x_{grn}) + f_{pos_d}(x_{cent})] - b_d & \text{if } \max[\cdot] > b_d, \text{ or} \\ 0 & \text{otherwise} \end{cases}, (18)$$

$$f_{negblupat_d}(x) = \begin{cases} \max[f_{neg_d}(x_{blu}) + f_{neg_d}(x_{grn}) + f_{neg_d}(x_{cent})] - b_d & \text{if } \max[\cdot] > b_d, \text{ or} \\ 0 & \text{otherwise} \end{cases}, (19)$$

$$f_{posblupat_d}(x) = \begin{cases} \max[f_{pos_d}(x_{blu}) + f_{pos_d}(x_{grn}) + f_{pos_d}(x_{cent})] - b_d & \text{if } \max[\cdot] > b_d, \text{ or} \\ 0 & \text{otherwise} \end{cases}, (20)$$

where  $f_{neg_d}(x_{red})$ ,  $f_{pos_d}(x_{red})$ ,  $f_{neg_d}(x_{grn})$ ,  $f_{pos_d}(x_{grn})$ ,  $f_{neg_d}(x_{blu})$ ,  $f_{pos_d}(x_{blu})$  are negative and positive functions of the local neighborhood red, green, and blue samples, except the center sample.

The negative and positive local neighborhood sample functions are

$$f_{neg_d}(x) = \sum_{n_1, n_2, p} w_{neg}[n_1, n_2, p, d] x[n_1, n_2], (21)$$

$$f_{pos_d}(x) = \sum_{n_1, n_2, p} w_{pos}[n_1, n_2, p, d] x[n_1, n_2], (22)$$

where  $p = 0, 1, \dots, P-1$  is the pattern index, and  $w_{neg}[\cdot]$ ,  $w_{pos}[\cdot] \in \{\sim 1, 1\}$  are sample weights, with  $\sim 1$  defined as the one's complement of the sample value in base-2, unsigned-binary representation. The sample 2D location indices  $n_1, n_2$  are restricted to values from  $0, 1, \dots, N-1$  where the required color sample is present in the mosaic.

The local neighborhood sample functions for red, green, blue, and center samples are

$$f_{neg_d}(x_{red}) = \sum_{n_1, n_2, p} w_{negred}[n_1, n_2, p, d] x_{red}[n_1, n_2], (23)$$

$$f_{pos_d}(x_{red}) = \sum_{n_1, n_2, p} w_{posred}[n_1, n_2, p, d] x_{red}[n_1, n_2], (24)$$

$$f_{neg_d}(x_{gm}) = \sum_{n_1, n_2, p} W_{neggm}[n_1, n_2, p, d] x_{gm}[n_1, n_2] \quad , \quad (25)$$

$$f_{pos_d}(x_{gm}) = \sum_{n_1, n_2, p} W_{posgm}[n_1, n_2, p, d] x_{gm}[n_1, n_2] \quad , \quad (26)$$

$$f_{neg_d}(x_{blu}) = \sum_{n_1, n_2, p} W_{negblu}[n_1, n_2, p, d] x_{blu}[n_1, n_2] \quad , \quad (27)$$

$$f_{pos_d}(x_{blu}) = \sum_{n_1, n_2, p} W_{posblu}[n_1, n_2, p, d] x_{blu}[n_1, n_2] \quad , \quad (28)$$

$$f_{neg_d}(x_{cent}) = \begin{cases} W_{negred} \left[ \frac{N-1}{2}, \frac{N-1}{2}, d \right] x_{red} \left[ \frac{N-1}{2}, \frac{N-1}{2} \right] & \text{for red center sample,} \\ W_{neggm} \left[ \frac{N-1}{2}, \frac{N-1}{2}, d \right] x_{gm} \left[ \frac{N-1}{2}, \frac{N-1}{2} \right] & \text{for green center sample, or } , (29) \\ W_{negblu} \left[ \frac{N-1}{2}, \frac{N-1}{2}, d \right] x_{blu} \left[ \frac{N-1}{2}, \frac{N-1}{2} \right] & \text{for blue center sample} \end{cases}$$

$$f_{pos_d}(x_{cent}) = \begin{cases} W_{posred} \left[ \frac{N-1}{2}, \frac{N-1}{2}, d \right] x_{red} \left[ \frac{N-1}{2}, \frac{N-1}{2} \right] & \text{for red center sample} \\ W_{posgm} \left[ \frac{N-1}{2}, \frac{N-1}{2}, d \right] x_{gm} \left[ \frac{N-1}{2}, \frac{N-1}{2} \right] & \text{for green center sample, or } .(30) \\ W_{posblu} \left[ \frac{N-1}{2}, \frac{N-1}{2}, d \right] x_{blu} \left[ \frac{N-1}{2}, \frac{N-1}{2} \right] & \text{for blue center sample} \end{cases}$$

The sample 2D location indices  $n_1, n_2$  are restricted to values from  $0, 1, \dots, N-1$  where the corresponding color sample value is present in the mosaic.

Sets of local sample patterns for a 3 x 3-local-neighborhood Bayer mosaic are shown in Figures 1 through 8. Each figure shows patterns for one of the eight possible input-output configurations of this mosaic. This number of configurations arises from the four different Bayer color sample types:

- Red samples (R),
- Green samples in rows with red samples (GR),
- Green samples in rows with blue samples (GB),
- Blue samples (B),

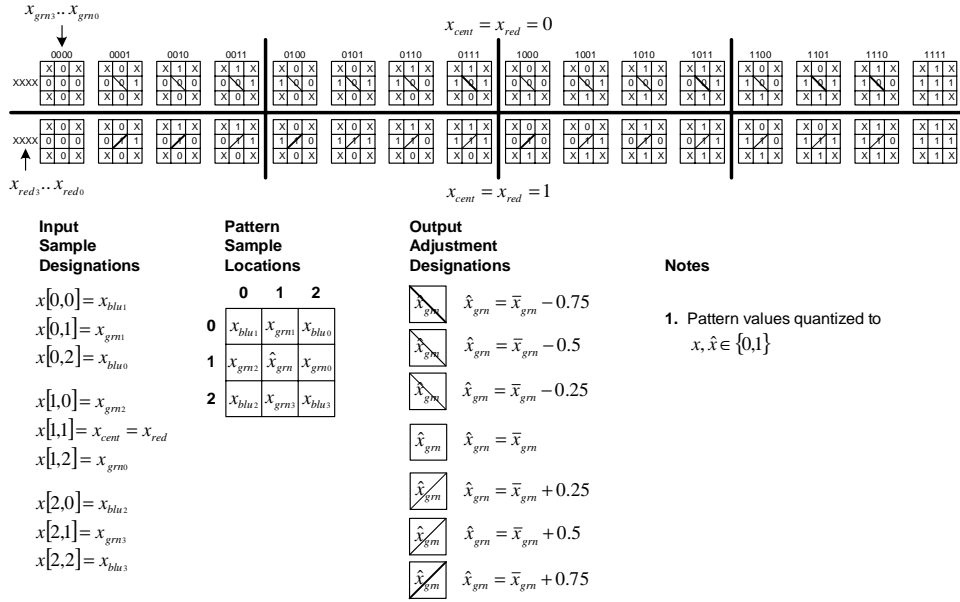


Fig. 1 Bayer RGB 3 x 3 R-Center G-Output patterns.

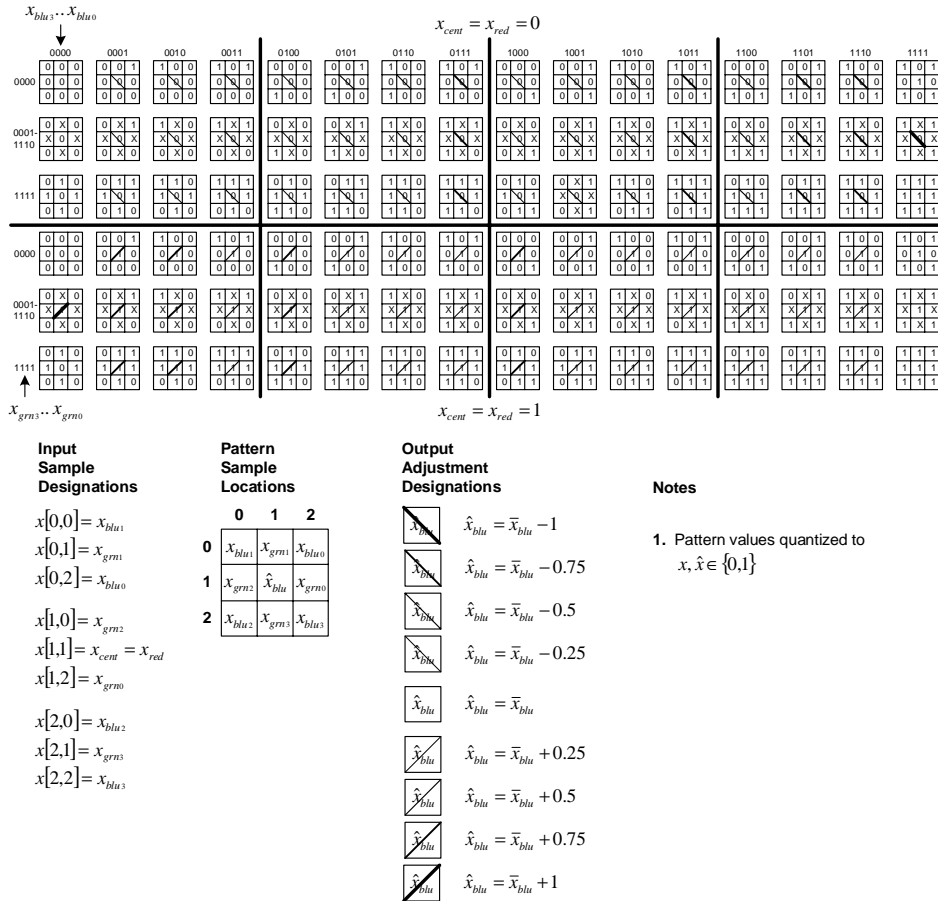


Fig. 2 Bayer RGB 3 x 3 R-Center B-Output patterns.

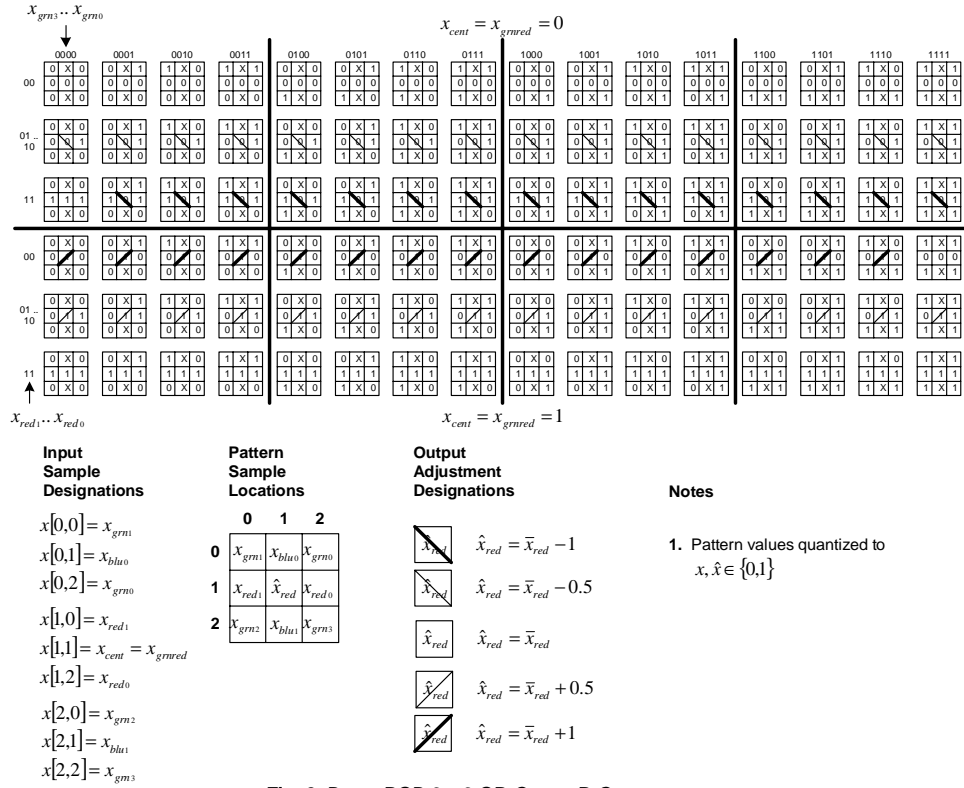


Fig. 3 Bayer RGB 3 x 3 GR-Center R-Output patterns.

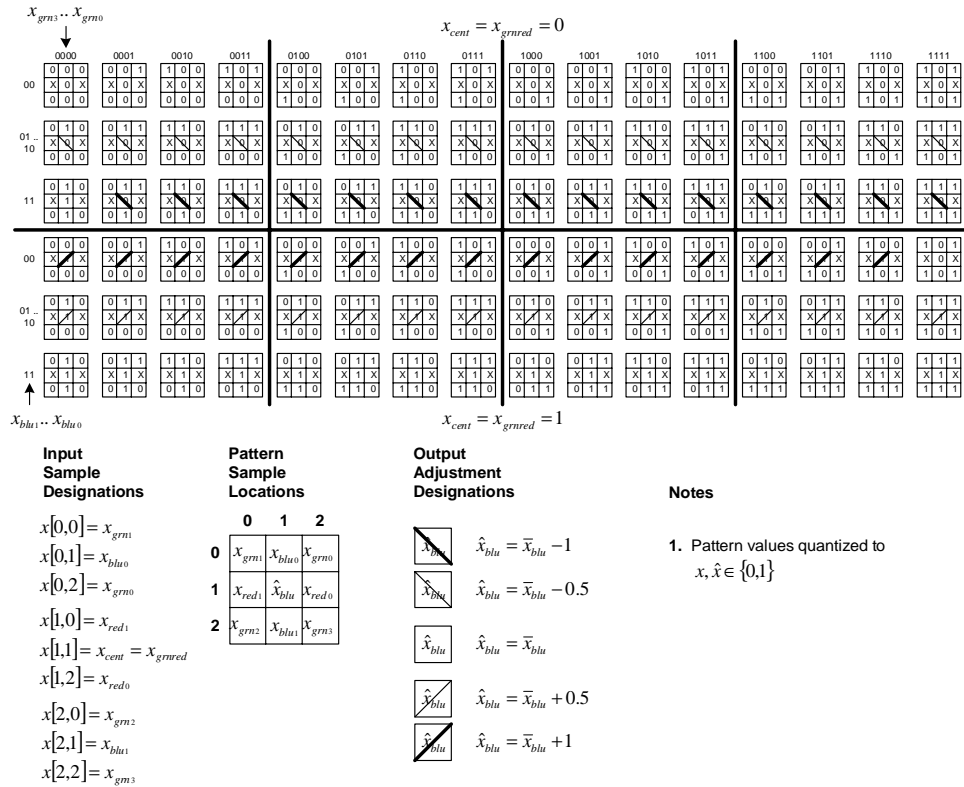


Fig. 4 Bayer RGB 3 x 3 GR-Center B-Output patterns.



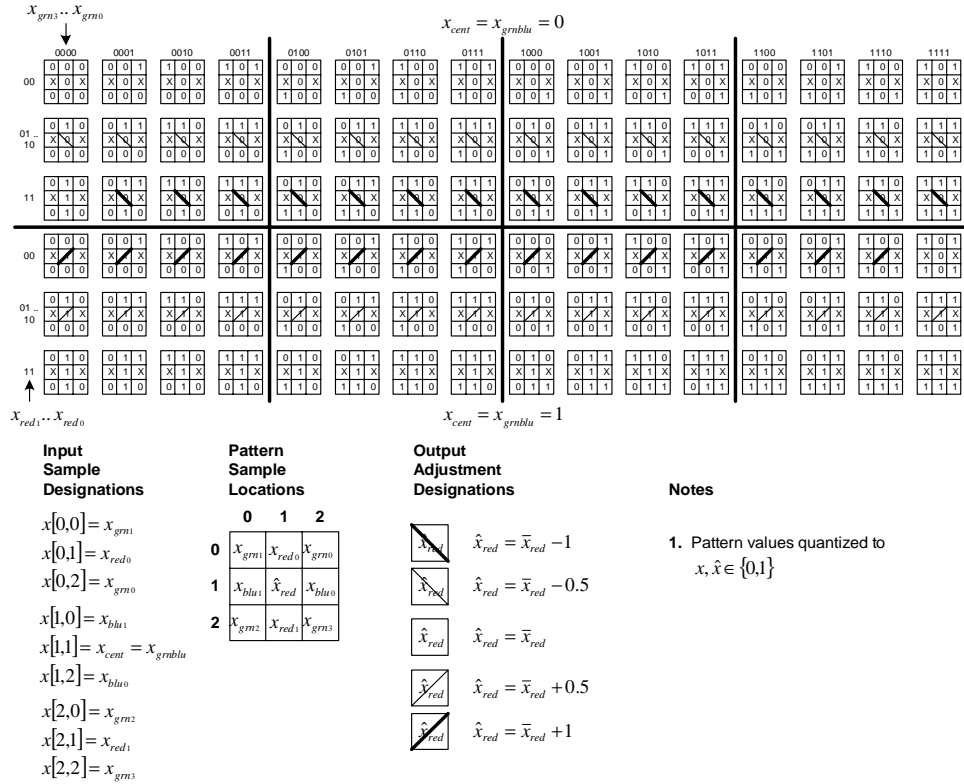


Fig. 5 Bayer RGB 3 x 3 GB-Center R-Output patterns.

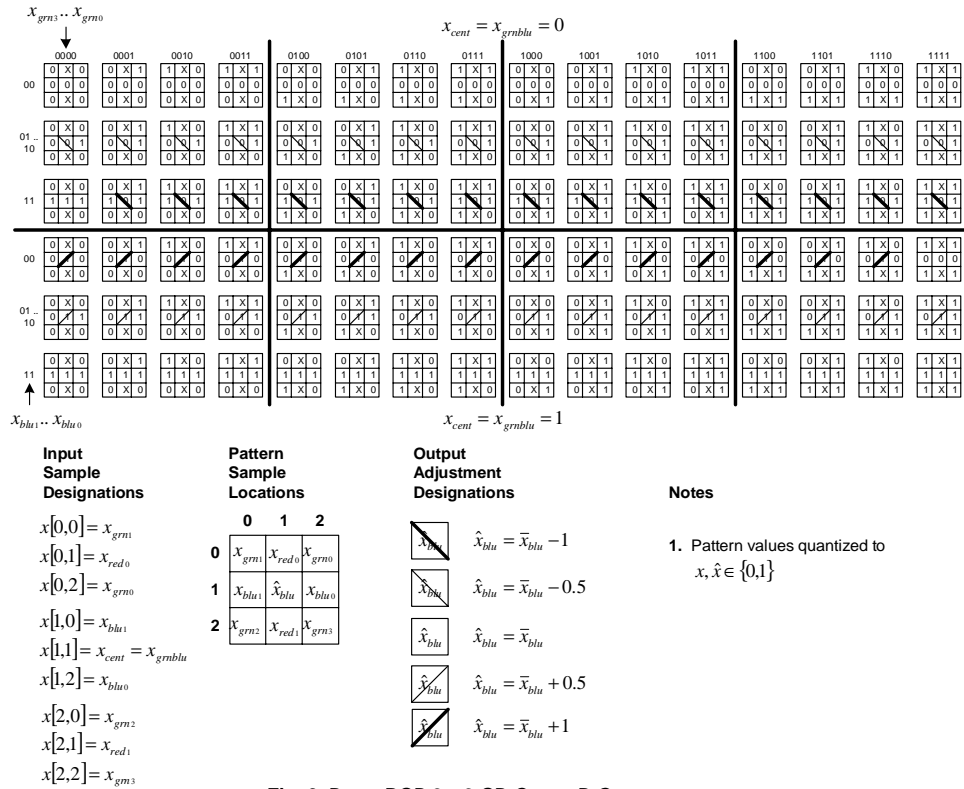


Fig. 6 Bayer RGB 3 x 3 GB-Center B-Output patterns.

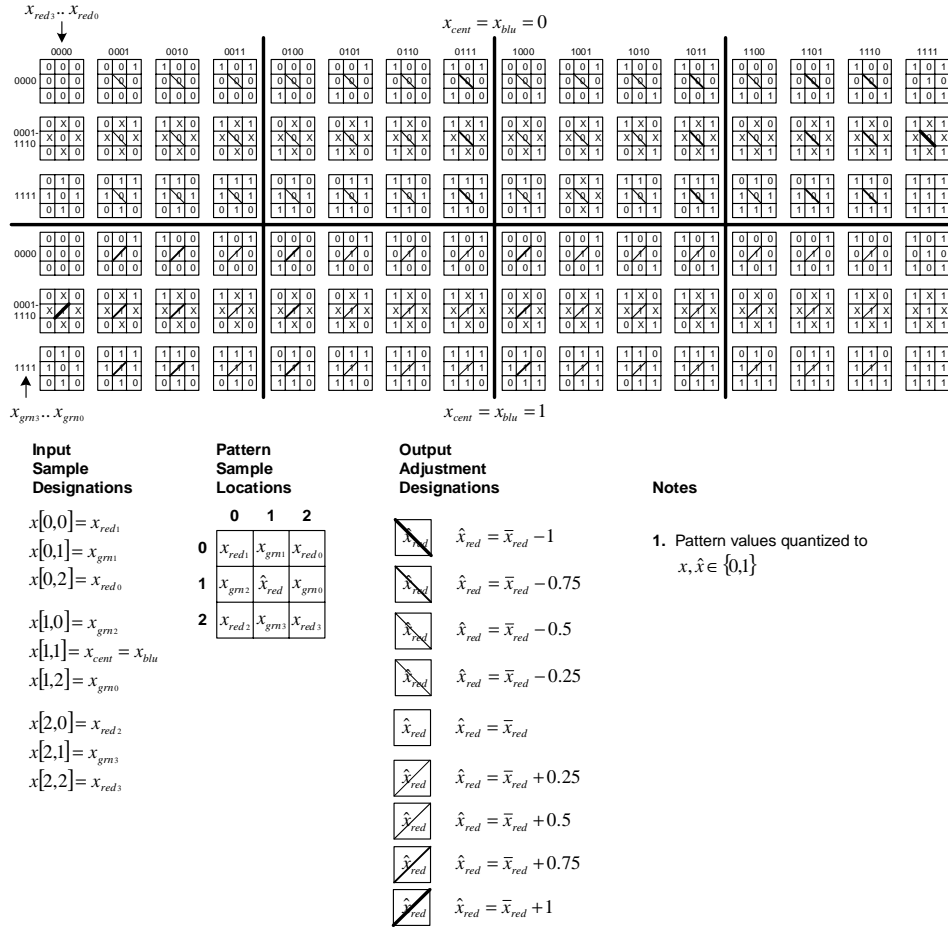


Fig. 7 Bayer RGB 3 x 3 B-Center R-Output patterns.

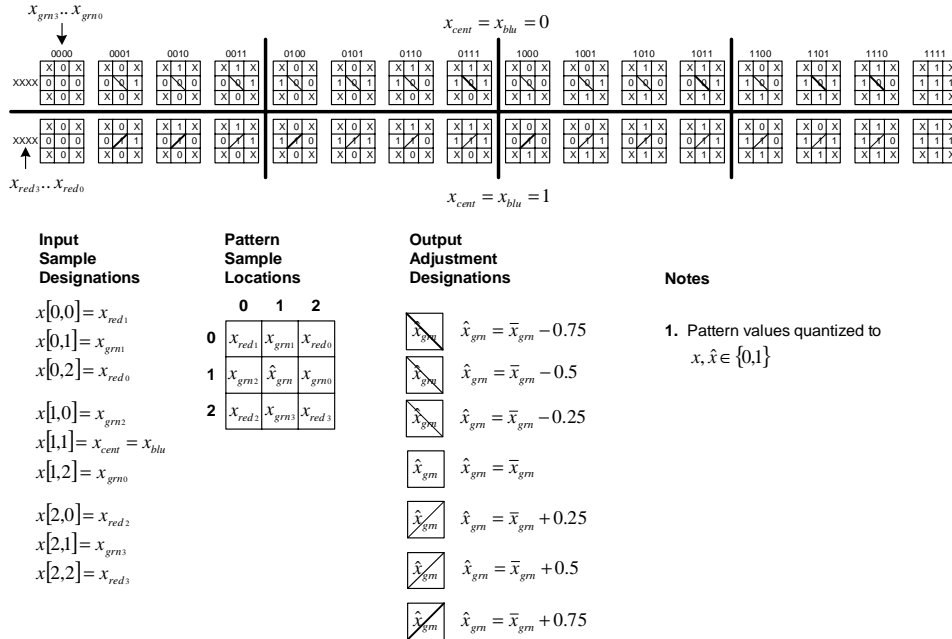


Fig. 8 Bayer RGB 3 x 3 B-Center G-Output patterns.

each centered in the 3 x 3 pattern, and each having two interpolated center color outputs. The patterns grouped according to their center sample colors are

R-Center Patterns	=	{ R-Center G-Output Patterns, R-Center B-Output Patterns },	(Fig. 1) (Fig. 2)
GR-Center Patterns	=	{ GR-Center R-Output Patterns, GR-Center B-Output Patterns },	(Fig. 3) (Fig. 4)
GB-Center Patterns	=	{ GB-Center R-Output Patterns, GB-Center B-Output Patterns },	(Fig. 5) (Fig. 6)
B-Center Patterns	=	{ B-Center R-Output Patterns, B-Center G-Output Patterns }.	(Fig. 7) (Fig. 8)

The pattern number,  $P$ , is equal to the total number of input-output configurations, so  $P = 8$  for this case.

The figures show the patterns using a notation  $x, \hat{x} \in \{0,1\}$ , where  $x, \hat{x} = 0$  represents the smallest value,  $x, \hat{x} = 1$  represents the largest value, and  $x = X$  represents a value of input sample  $x$  that is irrelevant to the interpolated color output value  $\hat{x}$ . The  $\hat{x}$  output values shown in the patterns are assigned according to the assumptions above. For a center sample value of either  $x = 0$  or  $x = 1$  in the patterns, the output  $\hat{x}$  is assigned a value of either  $\hat{x} = 0$  or  $\hat{x} = 1$ , such that  $\hat{x}$  is equal to the center sample value when the pattern shows a large luminance gradient.

The figures also show, using a diagonal line notation, the assigned values of  $\tilde{x}_{neg}$  and  $\tilde{x}_{pos}$ , the degree and direction of adjustment to the bilinear-interpolated values,  $\bar{x}$ . The diagonal lines indicate the different degrees and directions of adjustment using different line thicknesses and slopes. The line thickness is proportional to the degree of adjustment, and the line slope direction (positive or negative) is the same as the adjustment direction. For no adjustment; *i.e.*,  $\tilde{x}_{neg}, \tilde{x}_{pos} = 0$ , no line is shown.

The degree and direction of adjustment are defined from the pattern sample values as the difference between the assigned output value and the bilinear-interpolated value, shown by rearranging Equation 1 as

$$\tilde{x}_{neg} = \begin{cases} |\hat{x} - \bar{x}| & \text{for } \hat{x} - \bar{x} < 0, \text{ or} \\ 0 & \text{otherwise} \end{cases} \quad \text{and} \quad (31)$$

$$\tilde{x}_{pos} = \begin{cases} |\hat{x} - \bar{x}| & \text{for } \hat{x} - \bar{x} > 0, \text{ or} \\ 0 & \text{otherwise} \end{cases} \quad (32)$$

For sample pattern values quantized to  $x, \hat{x} \in \{0,1\}$  as shown in Figures 1 through 8, the possible bilinear-interpolated output values are  $\bar{x} \in \{0, 0.25, 0.5, 0.75, 1\}$ . The possible adjustment values are therefore (from Equations 31 and 32)  $\tilde{x}_{neg}, \tilde{x}_{pos} \in \{0, 0.25, 0.5, 0.75, 1\}$ . These values determine the adjustment weights  $w_{negpat_d}$  and  $w_{pospat_d}$  values in Equations 5 and 6, as follows.  $w_{negpat_d}$  and  $w_{pospat_d}$  are defined as equal to the change in  $\tilde{x}_{neg_d}$  and  $\tilde{x}_{pos_d}$  versus the change in the input sample pattern functions  $f_{negpat}(x)$  and  $f_{pospat}(x)$ , shown by rearranging Equations 5 and 6 as

$$w_{negpat_d} = \frac{\tilde{x}_{neg_d}}{f_{negpat_d}(x)} \quad \text{and} \quad (33)$$

$$W_{pospat_d} = \frac{\tilde{x}_{pos_d}}{f_{pospat_d}(x)} \quad . \quad (34)$$

The  $\tilde{x}_{neg}$  and  $\tilde{x}_{pos}$  values above are equal to the change in  $\tilde{x}_{neg}$  and  $\tilde{x}_{pos}$  over the full range of  $f_{negpat}(x)$  and  $f_{pospat}(x)$ , as produced by the entire range of associated input values, from the full pattern value, to the full complement of the same pattern value. Therefore, the  $W_{negpat_d}$  and  $W_{pospat_d}$  values are numerically equivalent to the  $\tilde{x}_{neg_d}$  and  $\tilde{x}_{pos_d}$  values, *i.e.*,  $W_{negpat_d}, W_{pospat_d} = \tilde{x}_{neg_d}, \tilde{x}_{pos_d} \in \{0, 0.25, 0.5, 0.75, 1\}$ . Also, the dimension number  $D$  is equal to the total number of  $\tilde{x}_{neg_d}$  or  $\tilde{x}_{pos_d}$  values. For the 3 x 3 Bayer mosaic under consideration,  $D = 5$ .

For each different adjustment degree and direction  $\tilde{x}_{neg_d}$  and  $\tilde{x}_{pos_d}$  shown in the figures, separate input-output transfer function equations are developed from the pattern values, as given by Equations 21 and 22. These equations are then algebraically reduced to minimized equations, as follows. With the pattern input values already quantized to  $x \in \{0, 1\}$ , the pattern adjustment output values are likewise quantized to  $\tilde{x} \in \{0, 1\}$ , with  $\tilde{x}$  set to  $\tilde{x} = 1$  for any non-zero  $\tilde{x}$  value, and set to  $\tilde{x} = 0$  otherwise. This allows the use of standard Boolean algebraic minimization techniques to minimize the equations. The outputs of the minimized equations are summed and thresholded as shown in Equations 13 and 14. These equation outputs are then scaled by their particular  $W_{negpat_d}$  and  $W_{pospat_d}$  values, and either added to or subtracted from the bilinear-interpolated value  $\tilde{x}$  to form the final output value  $\hat{x}$ , as shown by Equations 1, 5, and 6.

Examination of Figures 1 through 8 reveals that out of the eight different input-output configurations, only three unique pattern sets exist. Grouping together identical pattern sets, the three groups of unique pattern sets are

Patterns Group 1	=	{ R-Center G-Output Patterns, B-Center G-Output Patterns },	(Fig. 1) (Fig. 8)
Patterns Group 2	=	{ R-Center B-Output Patterns, B-Center R-Output Patterns },	(Fig. 2) (Fig. 7)
Patterns Group 3	=	{ GR-Center R-Output Patterns, GR-Center B-Output Patterns, GB-Center R-Output Patterns, GB-Center B-Output Patterns }.	(Fig. 3) (Fig. 4) (Fig. 5) (Fig. 6)

This grouping allows the total number of interpolation kernels to be restricted to three, the total number of unique pattern sets. The patterns shown according to their group designations are

R-Center Patterns	=	{ R-Center G-Output Patterns, R-Center B-Output Patterns },	(Group 1) (Group 2)
GR-Center Patterns	=	{ GR-Center R-Output Patterns, GR-Center B-Output Patterns },	(Group 3) (Group 3)
GB-Center Patterns	=	{ GB-Center R-Output Patterns, GB-Center B-Output Patterns },	(Group 3) (Group 3)
B-Center Patterns	=	{ B-Center R-Output Patterns, B-Center G-Output Patterns }.	(Group 2) (Group 1)

This grouping indicates a requirement for two sets of hardware implementing the Group 3 pattern interpolation, in order to concurrently obtain the two interpolated center color values of the GR-center and GB-center configurations.

### 3. RESULTS

The procedure was simulated using The MathWorks MATLAB® with the Lighthouse true-color (RGB, 8 bits-per-color) test image.<sup>15</sup> This image was decimated and converted from a 512 x 768 Tagged Image File Format image to a 256 x 384 Microsoft Windows® Bitmap image (Figure 9). The image was reduced to a Bayer RGB color mosaic image by removing the appropriate two color samples at each sample location (Figure 10). This color mosaic image was then interpolated in an attempt to recover the removed color samples. The resulting interpolated images were perceptually examined for image quality and interpolation artifacts.



Fig. 9: Lighthouse image



Fig. 10: Lighthouse Bayer RGB mosaic.

Figure 11 shows the bilinear-interpolated image with no adjustment. Figure 12 shows the bilinear-interpolated image with adjustment, using empirically obtained activation threshold bias  $b_d$  values. The bias values were perceptually adjusted to approximately optimal values. Values set too high resulted in insufficient adjustment, with the image exhibiting excessive color fringes. Values set too low resulted in excessive adjustment, with the image exhibiting “checkerboard” artifacts. All adjusted images shown here use the same bias values.



Fig. 11: Lighthouse bilinear-interpolated.



Fig. 12: Lighthouse bilinear-interpolated and adjusted.

In Figure 12, some color fringe reduction and image sharpening are present, but the image still contains substantial amounts of color fringes, as well as “zipper noise” artifacts and false colors. Another method for the bilinear interpolation was tried to improve the resultant image. The new method interpolated the image using the sample pattern values to direct the bilinear interpolation of colors having four samples in the local neighborhood. For these colors, the interpolation is selected from either the average of one of the two pairs of opposite-positioned samples, or the average of all four samples. The interpolation direction is chosen based on the similarity of the sample values to the pattern values, with each pattern value associated with a preferred interpolation direction. The pattern values and interpolation directions are associated through the correlations of the pattern values. Pattern values with a high degree of correlation in a particular direction are associated with interpolation in that direction. The adjustment weights are modified depending on whether the selected interpolation uses two samples or four samples. Figure 13 shows the interpolated image using the new interpolation method, but without adjustment, and Figure 14 shows the same image with adjustment. Some reduction in artifacts can be seen with this method, but the image still contains significant amounts of false colors.



Fig. 13: Lighthouse directed-linear-interpolated.



Fig. 14: Lighthouse directed-linear-interpolated and adjusted.

To reduce the false colors, median filtering of the red and blue color values, referenced to the green values, was used on the interpolated and adjusted image.<sup>16</sup> The median values of the color value differences (red – green) and (blue – green) were determined over the local neighborhood and added to the center green value to obtain new center red and blue values. These new red and blue values replaced the existing values. Figure 15 shows the results of this operation. The false colors are noticeably reduced.



Fig. 15: Lighthouse directed-linear-interpolated, adjusted, and median-filtered.

#### 4. CONCLUSION

This paper describes a methodology for color demosaicing using a data-driven connectionist approach. This methodology provided visible improvements over linear interpolation procedures. Although this paper presents the methodology in conjunction with bilinear interpolation, in theory it may be used in conjunction with other interpolation types to improve the resultant image quality.

The methodology uses only simple integer and logical operations over a small local sample neighborhood, thus facilitating its hardware implementation, especially for real-time pixel-rate hardware. As currently defined, the methodology requires only binary shifts, complementation, addition, comparison, and data selection, all having fairly simple hardware implementations. Iterative, recursive, or learning operations are not required.

Goals for future investigation include: Development of a more theoretical foundation for the methodology, performance optimization for general images or for special classes of images, optimization for hardware implementation, and implementation of the optimized procedure in hardware. Topics for future investigation include:

- Optimization of activation threshold bias values for the adjustment function.
- Nonlinear activation functions (*e.g.*, sigmoid function) for the adjustment.
- Larger local neighborhoods; *e.g.*,  $5 \times 5$  samples. The primary disadvantage of larger neighborhoods is the large increase in the procedure's design complexity and computational requirements.
- Theoretical links to wavelet-based image reconstruction. The methodology bears a semblance to wavelet or "wavelet-like" image reconstruction. The linear interpolation resembles low-frequency



signal recovery through a Haar scaling function, and the adjustment to the linear interpolation resembles high-frequency signal recovery through a Haar wavelet function.<sup>17</sup>

- Interactions with characteristics of the image acquisition process and with characteristics of other image processing functions.
- Combinations of this methodology with other color mosaic interpolation methodologies. One proposed application of this methodology is for providing a final “correction of last resort” to an image previously processed by another interpolation methodology.

## ACKNOWLEDGMENTS

The author would like to thank Dr. Todd Sachs of Agilent Technologies for his helpful suggestions and comments.

## REFERENCES

1. A. M. Tekalp, *Digital Video Processing*, Prentice Hall, Upper Saddle River, New Jersey (1995), Chap. 17.
2. T. Chen, “Spatial Color Interpolation Algorithms for Single-Detector Digital Cameras,” Psych221/EE362 Course Project, Image Systems Engineering Program, Department of Electrical Engineering, Stanford University (1999), <http://ise.stanford.edu/class/psych221/99/tingchen/>.
3. J. F. Hamilton and J. E. Adams, “Averaging green values for green photosites in electronic cameras,” United States Patent 5,596,367, Jan. 21, 1997.
4. J. E. Adams and J. F. Hamilton, “Adaptive color plane interpolation in single sensor color electronic camera,” United States Patent 5,652,621, Jul. 29, 1997.
5. R. Kimmel, “Demosaicing: Image Reconstruction from Color CCD Samples,” *IEEE Trans. Image Processing* **8**(9), 1221-1228 (1999).
6. S. B. Addison, “Method and system for color filter array multifactor interpolation,” United States Patent 5,990,950, Nov. 23, 1999.
7. D. D. Muresan, S. Luke, and T. W. Parks, “Reconstruction of Color Images from CCD Arrays”, Texas Instruments DSPS Fest 2000, Houston, Texas, (2000), <http://www.ti.com/sc/docs/general/dsp/festproceedings/fest2000/cornell001.pdf>.
8. M. R. Gupta and T. Chen, “Vector Color Filter Array Demosaicing,” *Proc. SPIE Sensors and Cameras Systems for Scientific, Industrial, and Digital Photography Applications III* **4306**, San Jose, California (2001).
9. F. Ahmed, S. C. Gustafson, and M. A. Karim, “High-Fidelity Image Interpolation using Radial Basis Function Neural Networks,” *Proc. IEEE 1995 Aerospace and Electronics Conf.* **2**, 588-592 (1995).
10. N. Plaziac, “Image Interpolation Using Neural Networks,” *IEEE Trans. Image Processing* **8**(11), 1647-1651 (1999).
11. F. M. Candocia and J. C. Principe, “Superresolution of Images Based on Local Correlations,” *IEEE Trans. Neural Networks* **10**(2), 372-380 (1999), [http://www.eng.fiu.edu:90/candocia/Personal/Publications/candocia\\_IEEE\\_TNN.pdf](http://www.eng.fiu.edu:90/candocia/Personal/Publications/candocia_IEEE_TNN.pdf).
12. J. Go, K. Sohn, and C. Lee, “Interpolation Using Neural Networks for Digital Still Cameras,” *IEEE Trans. Consumer Electronics* **46**(3), 610-616 (2000).
13. B. E. Bayer, “Color imaging array,” United States Patent 3,971,065, Jul. 20, 1976.
14. J. Adams, K. Parulski, and K. Spaulding, “Color Processing in Digital Cameras,” *IEEE Micro* **18**(6), 20-30 (1998).
15. The School of Electrical and Computer Engineering, Cornell University, Thomas Parks Digital Signal Processing Lab, Color Images Database, [http://texas.ee.cornell.edu/image/database/color/structures/000\\_512.tif](http://texas.ee.cornell.edu/image/database/color/structures/000_512.tif).
16. W. T. Freeman, “Method and apparatus for reconstructing missing color samples,” United States Patent 4,663,655, May 5, 1987.
17. E. J. Stollnitz, A. D. DeRose, and D. H. Salesin, *Wavelets for Computer Graphics: Theory and Applications*, Morgan Kaufmann, San Francisco (1996).